21st Australasian Fluid Mechanics Conference
Adelaide, Australia
10-13 December 2018

Extensional-flow theory with application to fibre drawing.

Y. M. Stokes[1]

[1]School of Mathematical Sciences, The University of Adelaide, South Australia 5005, Australia

Abstract

Extensional or elongational flows are most commonly associated with the study of rheology following the work of Trouton (1906). In this paper we outline an asymptotic method for the derivation of an extensional-flow model for the drawing of fibres. We obtain ODEs describing the change in area of the cross-section and the temperature from preform to fibre. In general, these are coupled with a 2D transverse-flow problem describing the evolution of the geometry in the cross-section due to surface tension and pressure. The accuracy of the model is demonstrated by comparison with experiments and finite-element simulations, and its computational efficiency is briefly discussed. Models may be obtained for other extensional flows using similar methods.

Introduction

Honey dripping from a spoon is an extensional (or elongational) flow; gravity causes the fluid to stretch. Such flows are ubiquitous in nature and industry and include fibre drawing (or spinning), the float glass process used for making sheet glass, and a spider spinning a web. Extensional flows are also used in rheometry to measure the extensional viscosity of liquids. Trouton is the father of extensional rheometry, publishing in 1906 [18] two theoretical explanations and results from experiments (including application of a tensile force to a rod of viscous fluid and gravitational spinning of a fluid thread) which showed the extensional viscosity of a Newtonian fluid to be three times its shear viscosity. Today the extensional viscosity for a Newtonian fluid is often called the Trouton viscosity and the ratio of the extensional and shear viscosities is called the Trouton ratio.

The Trouton ratio is readily derived by considering, as did Trouton [18], the elongation of a uniform cylinder of (essentially) incompressible isotropic viscous fluid, assuming the rate of elongational strain to be uniform in any cross-section. Concurrently with elongation at rate e it must contract at rate $e/2$ in the transverse directions. Setting x to be the axis along which elongation occurs, and y and z to be the transverse directions, the rate-of-strain tensor is

$$E = \begin{pmatrix} e & 0 & 0 \\ 0 & -e/2 & 0 \\ 0 & 0 & -e/2 \end{pmatrix} \qquad (1)$$

and the stress tensor is $\Sigma = -pI + 2\mu E$, where p is pressure, μ is the shear viscosity, and I is the 3×3 identity matrix. On the free surface of the cylinder we set the stress to be zero, i.e. $\Sigma_{22} = \Sigma_{33} = 0$, giving $p = -\mu e$. Then the elongational stress is $\Sigma_{11} = -p + 2\mu e = 3\mu e = \mu_T e$ and we have that the extensional viscosity μ_T is three times the shear viscosity. A flow in which the only non-zero components in the rate-of-strain tensor are on the main diagonal, as in (1), is called a pure extensional flow.

Figure 1 shows a schematic of an essentially steady-state process for the drawing of a long fibre. A thread of viscous fluid or preform with temperature θ_{in} and cross-sectional area χ^2_{in} is fed through an aperture at $x = 0$ at a slow feed speed U_{in}. At a distance L from the aperture, the thread is pulled at a much larger draw speed U_{out} by a take-up roller. Between $x = 0$ and

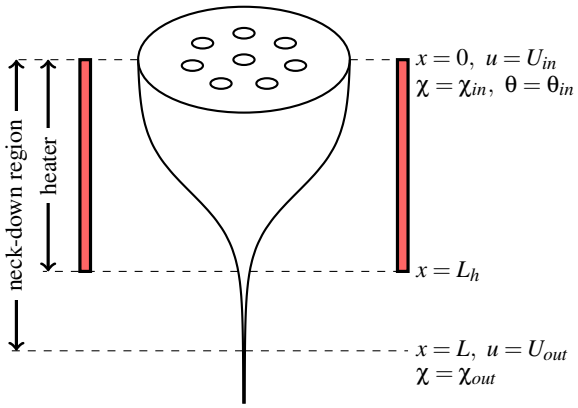

Figure 1: Schematic diagram of the neck-down region, $0 \le x \le L$, over which the initial cross-sectional area of the thread χ^2_{in} reduces to that of the fibre χ^2_{out} due to the large draw speed U_{out} relative to the feed speed U_{in}.

$x = L_h < L$ the thread is heated and, from $x = L_h$ to $x = L$ it cools to a solid. At the aperture the cross-section of the thread may, as in the case of microstructured optical fibres, contain a pattern of air channels and over the so-called *neck-down* region $0 \le x \le L$ the thread deforms greatly due primarily to the *draw ratio* $D = U_{out}/U_{in} \gg 1$ which results in reduction of the cross-sectional area χ^2 with x; surface tension and/or any pressure applied within the channels, also deforms the geometry. By mass conservation the cross-sectional area at $x = L$ is $\chi^2_{out} = \chi^2_{in}/D$. This is the illustrative extensional-flow problem for this paper although the methods are readily extended, for example, to the unsteady problems of stretching a viscous fluid thread by extending both ends [20] and the slow dripping under gravity of a viscous fluid from a tube [19, 17].

Motivated by the spinning of textile fibres, such as nylon, and the blowing of tubular plastic film, Pearson and coworkers [10, 12, 13] were pioneers in the modelling of these types of flows, using asymptotic methods to derive extensional-flow models under the assumption of an axisymmetric geometry. Much work followed, only a little of which can be mentioned here. Wilson [19] used force-balance arguments to derive a model for the dripping of a viscous fluid from a tube. A general formal derivation of the leading-order extensional-flow model for the drawing of non-axisymmetric viscous fibres with surface tension considered negligible was done by Dewynne and others [5, 6], while Cummings and Howell [4] extended this work to non-negligible surface tension. In more recent times in the context of the drawing of microstructured optical fibres the work has been extended to tubes [7, 8] and fibres of arbitrary cross-sectional shape [1, 2, 15].

As shown in [2, 15], if only the final geometry of the fibre is important but the evolution of that geometry along the neck-down length is not important, and all material properties other than the viscosity are constant, then temperature modelling is not necessary. It is the harmonic mean of the viscosity over the neck-down length, which determines the tension along the fi-

bre (and vice versa), that determines the shape of fibre obtained from some initial preform geometry. Any temperature profile that gives the same fibre tension and, hence, harmonic mean of the viscosity, will result in the same fibre geometry from a given initial geometry. It is, however, necessary that the fibre tension can be measured and controlled (by adjusting the heater temperature) during a fibre draw. If this is not the case or knowledge of the geometry along the neck-down length is desired then temperature modelling becomes necessary. The aim of this paper is to couple a temperature model to the flow-only model for fibre drawing of [2] and, in the process, to demonstrate asymptotic methods for derivation of extensional-flow models. Another paper is in preparation dealing with coupled flow and temperature modelling in the case of temperature-dependent viscosity and surface tension when temperature modelling becomes essential just to determine the fibre geometry [16].

Model derivation

The derivation of extensional-flow models for problems of interest here exploit the fact that the geometry is slender, i.e. the axial length scale (in the direction of stretching) is much larger than the width. An important consequence is that the axial component of velocity, the pressure and the temperature are approximately uniform in any cross-section which, in turn, permits derivation of a much simpler model than would otherwise be possible. This will be seen in the context of the fibre-draw problem shown in figure 1. It is not uncommon to simply start by assuming the uniformity of these quantities in the cross-section, however, we will not do this here but outline how this and the final model may be derived using asymptotic methods; for more details see [2, 4, 5, 6, 16].

Let $\boldsymbol{x} = (x,y,z)$ denote position, with stretching in the direction of the x-axis (see figure 1), $\boldsymbol{u} = (u,v,w)$ be the velocity vector, p be the pressure, and θ be the temperature. We start by considering that the dependent variables are, in general, functions of position $\boldsymbol{x}$ and time t. We suppose that all fluid properties are constant with the exception of the viscosity $\mu(\theta)$ which is a known function of temperature. We denote the shape of the external boundary of the thread by $G^{(0)}(\boldsymbol{x},t) = 0$ and the shape of each of the N internal holes to be $G^{(i)}(\boldsymbol{x},t) = 0$, $i = 1,2,\ldots,N$. The outward pointing normal vectors on the boundaries are, hence, denoted by $\boldsymbol{n}^{(i)} = \boldsymbol{\nabla} G^{(i)}/|\boldsymbol{\nabla} G^{(i)}|$. Recall that the cross-sectional area at axial position x and time t is $\chi^2(x,t)$ and, for convenience, we also define $\Gamma(x,t)$ to be the total length of all of its boundaries. For our illustrative problem $\chi(0,t) = \chi_{in}$, $\Gamma(0,t) = \Gamma_{in}$, and the shapes of the external boundary and the internal holes at the aperture are denoted by $G^{(0)}_{in}(y,z) = 0$ and $G^{(i)}_{in}(y,z) = 0$, respectively.

Full model

Assuming an incompressible Newtonian fluid, the governing equations for the fluid flow are

$$\boldsymbol{\nabla}\cdot\boldsymbol{u} = 0, \tag{2a}$$

$$\rho\left(\frac{\partial \boldsymbol{u}}{\partial t} + \boldsymbol{u}\cdot\boldsymbol{\nabla}\boldsymbol{u}\right) = -\boldsymbol{\nabla} p + \boldsymbol{\nabla}\cdot\left(\mu(\theta)\left(\boldsymbol{\nabla}\boldsymbol{u} + (\boldsymbol{\nabla}\boldsymbol{u})^T\right)\right), \tag{2b}$$

where ρ is the density of the fluid. On the external surface of the cylinder and on the N internal surfaces, the dynamic and kinematic boundary conditions are

$$-p\boldsymbol{n}^{(i)} + \mu(\theta)\left(\boldsymbol{\nabla}\boldsymbol{u} + (\boldsymbol{\nabla}\boldsymbol{u})^T\right)\cdot\boldsymbol{n}^{(i)} = -(\gamma\kappa^{(i)} + p^{(i)})\boldsymbol{n}^{(i)}, \tag{2c}$$

$$\frac{\partial G^{(i)}}{\partial t} + \boldsymbol{u}\cdot\boldsymbol{\nabla} G^{(i)} = 0, \tag{2d}$$

for $i = 0,1,\ldots,N$, where $\kappa^{(i)}$ is the local curvature of the ith boundary, γ is the surface tension coefficient, $p^{(0)} = 0$ is the ambient air pressure and $p^{(i)} = p_H$, $i = 1,\ldots,N$, is the constant pressure applied in the air channels. At $x = L$ the speed of the thread is controlled by the take-up roller and hence given by $u = U_{out}$.

Assuming the thread is heated and cooled radiatively and is optically thick for wavelengths that dominate the heat transfer, so that heating/cooling occurs only at the external boundary of the thread [11], the governing equation for the temperature θ is given by

$$\rho c_p\left(\frac{\partial\theta}{\partial t} + \boldsymbol{u}\cdot\boldsymbol{\nabla}\theta\right) = k\nabla^2\theta, \tag{3a}$$

where c_p and k are the specific heat and conductivity of the fluid, respectively. On the external boundary we have

$$-k\boldsymbol{\nabla}\theta\cdot\boldsymbol{n}^{(0)} = \begin{cases} k_b\beta\left(\theta^4 - \theta_h^4(x)\right), & 0 \le x \le L_h, \\ k_b\beta\left(\theta^4 - \theta_a^4\right), & L_h < x \le L, \end{cases} \tag{3b}$$

and on the internal boundaries

$$-k\boldsymbol{\nabla}\theta\cdot\boldsymbol{n}^{(i)} = 0, \quad i = 1,\ldots,N. \tag{3c}$$

Here k_b is the Stefan-Boltzmann constant, β is the absorptivity of the surface, θ_a is the constant ambient temperature beyond the heater, $\theta_h(x)$ is the temperature of the heater that, in general, will be spatially dependent, and we have assumed negligible heat transfer across internal cavities compared to the heat transfer at the external boundary.

Asymptotic model reduction

For our illustrative problem (figure 1) we now characterise the slenderness of the geometry by $\varepsilon = \chi_{in}/L$, where we have used the square root of the cross-sectional area at $x = 0$ as the characteristic length scale in the cross-section and the neck-down length as the axial length scale. To obtain a simplified extensional-flow model we assume that $\varepsilon \ll 1$ and define

$$(x,y,z) = L(x',\varepsilon y',\varepsilon z'), \quad t = \frac{L}{U_{in}}t', \quad p = \frac{\mu_{hot}U_{in}}{L}p',$$
$$(u,v,w) = U_{in}(u',\varepsilon v',\varepsilon w'), \quad \chi = \chi_{in}\chi', \quad \Gamma = \chi_{in}\Gamma',$$
$$\kappa = \kappa'/\chi_{in} \quad \theta = \theta_{in} + \Theta\theta', \quad \mu(\theta) = \mu_{hot}\mu'(\theta'),$$

where $\Theta = (\theta_{hot} - \theta_{in})$, $\theta_{hot} = \max_x\{\theta_h(x)\}$, $\mu_{hot} = \mu(\theta_{hot})$, and primes denote dimensionless variables. We also define the Reynolds, Péclet and capillary numbers and a dimensionless absorptivity as

$$\mathrm{Re} = \frac{\rho U_{in}L}{\mu_{hot}}, \quad \mathrm{Pe} = \frac{\rho c_p U_{in}L}{k}, \quad \mathrm{Ca} = \frac{\mu_{hot}U_{in}\chi_{in}}{\gamma L},$$
$$\mathcal{H}_R = \frac{\beta k_b\theta_{hot}^4\mu_{hot}}{\rho c_p\Theta\gamma},$$

respectively. Next we write our equations and boundary conditions in terms of the scaled variables, dropping time-dependence because our problem is steady, along with primes for convenience. In the interests of space we here give just the temperature equation,

$$\varepsilon^2\mathrm{Pe}\left(u\frac{\partial\theta}{\partial x} + v\frac{\partial\theta}{\partial y} + w\frac{\partial\theta}{\partial z}\right) = \varepsilon^2\frac{\partial^2\theta}{\partial x^2} + \frac{\partial^2\theta}{\partial y^2} + \frac{\partial^2\theta}{\partial z^2}, \tag{4a}$$

and the associated boundary condition on the external boundary,

$$-\left(\varepsilon^2\frac{\partial\theta}{\partial x}n_x^{(0)} + \boldsymbol{\nabla}_\perp\theta\cdot\boldsymbol{n}_\perp^{(0)}\right) = \frac{\varepsilon^2\mathrm{Pe}\mathcal{H}_R}{\mathrm{Ca}}f_R(\theta,x), \tag{4b}$$

noting that, for internal boundaries, the normal vector becomes $\boldsymbol{n}_\perp^{(i)}$ and the right-hand-side of (4b) simply becomes zero. Here $\boldsymbol{\nabla}_\perp$ and $\boldsymbol{n}_\perp^{(i)}$ denote the gradient and normal vectors in the $y-z$ plane, and

$$f_R(\theta,x) = \begin{cases} \big(\theta+\vartheta_{in}(1-\theta)\big)^4 - \big(\vartheta_h(x)\big)^4, & 0 \le x \le \ell, \\ \big(\theta+\vartheta_{in}(1-\theta)\big)^4 - \vartheta_a^4, & \ell < x \le 1, \end{cases}$$

where $\vartheta_{in} = \theta_{in}/\theta_{hot}$, $\vartheta_a = \theta_a/\theta_{hot}$, $\vartheta_h(x) = \theta_h(x)/\theta_{hot}$, and $\ell = L_h/L$. We also expand all dependent variables in powers of ε^2, for example,

$$\theta = \theta_0(x,y,z,t) + \varepsilon^2\theta_1(x,y,z,t) + \varepsilon^4\theta_2(x,y,z,t) + \ldots, \quad (5)$$

and substitute these into our equations. Substituting (5) into the temperature equation and boundary conditions, and taking the leading order terms gives

$$\nabla_\perp^2\theta_0 = 0,$$
$$\boldsymbol{\nabla}_\perp\theta_0\cdot\boldsymbol{n}_\perp^{(i)} = 0, \quad i = 0,1,\ldots,N,$$

which implies that $\theta_0 = \theta_0(x)$, i.e. at leading order temperature is uniform in a cross-section and, therefore, so too is the viscosity $\mu(\theta_0)$. Similarly it can be shown that $u_0 = u_0(x)$.

Returning to (4a) and (4b) we now take $O(\varepsilon^2)$ terms to obtain

$$\mathrm{Pe}\,u_0\frac{\partial\theta_0}{\partial x} = \frac{\partial^2\theta_0}{\partial x^2} + \frac{\partial^2\theta_1}{\partial y^2} + \frac{\partial^2\theta_1}{\partial z^2}, \quad (6a)$$

$$-\left(\frac{\partial\theta_0}{\partial x}n_x^{(0)} + \boldsymbol{\nabla}_\perp\theta_1\cdot\boldsymbol{n}_\perp^{(0)}\right) = \frac{\mathrm{Pe}\mathcal{H}_R}{\mathrm{Ca}}f_R(\theta_0,x). \quad (6b)$$

Again we note that the boundary conditions on internal boundaries are similar to (6b) but with a zero right-hand-side. Integrating (6a) over the cross-sectional area at axial position x and using the divergence theorem and the boundary conditions gives

$$u_0\chi_0^2\frac{d\theta_0}{dx} = \frac{1}{\mathrm{Pe}}\frac{d}{dx}\left(\chi_0^2\frac{d\theta_0}{dx}\right) - \frac{\mathcal{H}_R\Gamma_0^{(0)}}{\mathrm{Ca}}f_R(\theta_0,x), \quad (7)$$

where $\Gamma_0^{(0)}(x)$ is the leading-order length of the external boundary of the cross-section at x.

Similar, though somewhat more complex, methods as used to derive (7) are used to obtain an asymptotic ODE for the leading-order axial flow $u_0(x)$,

$$-\mathrm{Re}\chi_0^2u_0\frac{du_0}{dx} + \frac{d}{dx}\left(3\mu(\theta_0)\chi_0^2\frac{du_0}{dx}\right) + \frac{1}{2\mathrm{Ca}}\frac{d\Gamma_0}{dx} = 0, \quad (8)$$

where $\Gamma_0(x)$ is the leading-order total length of the external and internal boundaries of the cross-section at x. Since this is an extensional-flow model we, not surprisingly, see the appearance of the Trouton viscosity $3\mu(\theta_0)$ in this equation. The continuity equation yields

$$\frac{d}{dx}\left(u_0\chi_0^2\right) = 0 \quad \Rightarrow \quad u_0\chi_0^2 = 1, \quad (9)$$

which may be used to simplify (7) and (8), the latter of which may then be integrated. Noting that $\mathrm{Re} = O(10^{-8})$ and $Pe = O(10)$, we drop the inertial term in the flow equation and the second-order term in the temperature equation. From this we have

$$-6\mu(\theta_0)\frac{1}{\chi_0}\frac{d\chi_0}{dx} + \frac{1}{2\mathrm{Ca}}\Gamma_0 = 6T, \quad (10a)$$

$$\frac{d\theta_0}{dx} + \frac{\mathcal{H}_R\Gamma_0^{(0)}}{\mathrm{Ca}}f_R(\theta_0,x) = 0, \quad (10b)$$

where $6T$ is the constant (dimensionless) tension in the fibre.

Transverse flow model

Our reduced equations include $\Gamma_0(x)$ and $\Gamma_0^{(0)}(x)$, the leading-order lengths of all boundaries and the external boundary of the cross-section at x, respectively. In the case of zero surface tension ($\gamma = 0$) the cross-section changes in scale with x but not in shape so that $\Gamma_0(x) = \chi_0(x)\Gamma_0(0)$, $\Gamma_0^{(0)}(x) = \chi_0(x)\Gamma_0^{(0)}(0)$, and we simply make these substitutions in (10). However, for $\gamma \neq 0$, these boundary lengths must, in general, be found by solving for the transverse components (v,w) of the fluid flow. The model for this is derived from the leading-order terms of the scaled equations and dynamic boundary conditions for v and w, along with the kinematic boundary condition. By writing the flow in the cross-section as the sum of the solution in the absence of surface tension (denoted by subscripts Z) and a component due to surface tension (denoted by tildes),

$$p_0 = p_Z + \frac{1}{\mathrm{Ca}\chi_0}\tilde{p}, \quad (v_0,w_0) = (v_Z,w_Z) + \frac{1}{\mathrm{Ca}\mu(\theta_0)}(\tilde{v},\tilde{w}),$$

scaling the transverse coordinates, boundary lengths and curvature with $\chi_0(x)$,

$$(y,z) = \chi_0(\tilde{y},\tilde{z}), \quad \Gamma^{(i)} = \chi_0\tilde{\Gamma}^{(i)}, \quad \kappa^{(i)} = \tilde{\kappa}^{(i)}/\chi_0,$$

and employing the transformation from x to τ given by

$$\frac{d\tau}{dx} = \frac{\chi_0}{\mathrm{Ca}\mu(\theta_0)}, \quad \tau = 0 \text{ at } x = 0,$$

the flow in the cross-section due to surface tension is given by a classical 2D free-boundary Stokes-flow problem driven by unit surface tension in a domain of unit area, namely

$$\tilde{v}_{\tilde{y}} + \tilde{w}_{\tilde{z}} = 0, \quad (11a)$$
$$\tilde{v}_{\tilde{y}\tilde{y}} + \tilde{v}_{\tilde{z}\tilde{z}} = \tilde{p}_{\tilde{y}}, \quad (11b)$$
$$\tilde{w}_{\tilde{y}\tilde{y}} + \tilde{w}_{\tilde{z}\tilde{z}} = \tilde{p}_{\tilde{z}}, \quad (11c)$$

with boundary conditions on $G^{(i)}(\tau,\tilde{y},\tilde{z}) = 0$,

$$G_\tau^{(i)} + \tilde{v}G_{\tilde{y}}^{(i)} + \tilde{w}G_{\tilde{z}}^{(i)} = 0, \quad (11d)$$
$$(-\tilde{p} + 2\tilde{v}_{\tilde{y}})G_{\tilde{y}}^{(i)} + (\tilde{v}_{\tilde{z}} + \tilde{w}_{\tilde{y}})G_{\tilde{z}}^{(i)} = -(\tilde{\kappa}^{(i)} + \mathcal{P}^{(i)}\chi_0)G_{\tilde{y}}^{(i)}, \quad (11e)$$
$$G_{\tilde{y}}^{(i)}(\tilde{v}_{\tilde{z}} + \tilde{w}_{\tilde{y}}) + G_{\tilde{z}}^{(i)}(-\tilde{p} + 2\tilde{w}_{\tilde{z}}) = -(\tilde{\kappa}^{(i)} + \mathcal{P}^{(i)}\chi_0)G_{\tilde{z}}^{(i)}, \quad (11f)$$

where $\mathcal{P}^{(0)} = 0$ and $\mathcal{P}^{(i)} = \mathrm{Ca}\,p_HL/(\mu_{hot}U_{in})$, $i = 1,\ldots,N$. Here subscripts denote differentiation with respect to the subscript variables. The solution of this transverse flow problem yields both the scaled total boundary length $\tilde{\Gamma}$ and the scaled outer boundary length $\tilde{\Gamma}^{(0)}$ at each τ, as well as the cross-sectional geometry. We note that if the channels are not pressurised ($p_H = 0$) the cross-sectional flow problem completely decouples from the axial flow and temperature problems and may be solved first but, otherwise, there is full coupling and all must be solved simultaneously.

Extensional-flow model

To couple the cross-sectional flow problem with the temperature and axial flow equations it is convenient to write (10) in terms of τ. Our final model is (dropping the subscript zeros) the

remarkably simple system of first-order ODEs

$$\frac{d\chi}{d\tau} - \frac{1}{12}\chi\tilde{\Gamma} = -\mathcal{T}, \quad \mathcal{T} = T\,\mathrm{Ca}, \tag{12a}$$

$$\frac{d\theta}{d\tau} = -\frac{\mathcal{H}_R\mu(\theta)\tilde{\Gamma}^{(0)}}{\mathrm{Ca}} f_R(\theta,x), \tag{12b}$$

$$\frac{dx}{d\tau} = \frac{\mathrm{Ca}\,\mu(\theta)}{\chi}, \tag{12c}$$

with the boundary conditions $\chi(0)=1$, $\chi(1)=1/\sqrt{D}$, $\theta(0)=0$ and $x(0)=0$, along with the transverse flow problem. Note that the boundary condition for χ at $x=1$ is used to determine the tension parameter T.

Solution for an axisymmetric cylinder

We here consider the case of drawing an axisymmetric tube. Defining $\phi(\tau)$ to be the radius of the hole over the radius of the tube (i.e. the aspect ratio of the tube) at τ, and $\phi_{in}=\phi(0)$, the axisymmetric transverse flow problem yields [2]

$$\frac{d\alpha}{d\tau} = \begin{cases} \dfrac{1}{2} - \dfrac{\mathcal{P}}{8\pi}\left(\dfrac{1-\pi^2\alpha^4}{\alpha}\right)\chi, & \alpha < 1/\sqrt{\pi}, \\ 0, & \alpha \geq 1/\sqrt{\pi}, \end{cases} \tag{13}$$

with initial condition $\alpha(0)=\alpha_{in}$, where

$$\alpha(\tau) = \sqrt{\frac{1-\phi}{\pi(1+\phi)}} \quad \text{and} \quad \alpha_{in} = \sqrt{\frac{1-\phi_{in}}{\pi(1+\phi_{in})}}. \tag{14}$$

Note that $\alpha = 1/\sqrt{\pi}$ corresponds to $\phi=0$, i.e. closure of the hole, and typically we would choose the pressure parameter $\mathcal{P}$ to prevent this, although not so large as to cause $\alpha(\tau)$ to become zero at any τ, corresponding to bursting of the tube ($\phi(\tau)=1$). For an annulus of unit area and aspect ratio ϕ it is readily shown that

$$\tilde{\Gamma}(\tau) = \frac{2}{\alpha} \quad \text{and} \quad \tilde{\Gamma}^{(0)}(\tau) = \frac{1}{\alpha(\tau)} + \pi\alpha(\tau), \tag{15}$$

which we substitute into (12a) and (12b).

Thus we have a system of four coupled ODEs for $\chi(\tau)$, $\theta(\tau)$, $x(\tau)$ and $\alpha(\tau)$ which are readily solved using, for example, the "ode45" solver in Matlab. From these quantities we may compute the (dimensionless) radius $R(\tau)$ and the aspect radius $\phi(\tau)$ of the tube. For specified heater temperature profile $\vartheta_h(x)$, viscosity-temperature relation $\mu(\theta)$, tension $\mathcal{T}$ and pressure $\mathcal{P}$, solution is straight-forward but the desired cross-sectional area at $x=1$ (equivalently the draw ratio) may not be obtained. Thus we use a root-finding procedure, such as 'fzero' in Matlab, to determine the tension $\mathcal{T}$ that yields $\chi_0(1)=1/\sqrt{D}$.

Figures 2–5 show solutions for an axisymmetric tube obtained using four different channel pressurisations, as given in the captions. Also given in the captions are the values of T and $\phi_{out}=\phi|_{x=1}$, determined as part of the solution process. At $x=0$ the dimensional geometry is given by $\phi_{in}=0.2$ and $\chi_{in}=8.7\times10^{-3}$ m, so that the external radius is 5×10^{-3} m. The incoming velocity was set at $U_{in}=2.3\times10^{-5}\,\mathrm{m\,s^{-1}}$ and the draw ratio at $D=5000$, yielding $\chi_{out}=\chi_{in}/\sqrt{D}=1.23\times10^{-4}$ m. The dimensional temperature parameters were $\theta_{in}=650$ K, $\theta_a=290$ K, and $\theta_{hot}=1000$ K (yielding $\mu_{hot}=3.78\times10^4$ Pa s), the physical heater and neck-down lengths were $L_h=0.05$ m and $L=0.2$ m, respectively, and the dimensional heater profile, with temperature again in Kelvin, was specified as

$$\theta_h(x) = 950 + 200\frac{x}{L_h}\left(1-\frac{x}{L_h}\right), \tag{16}$$

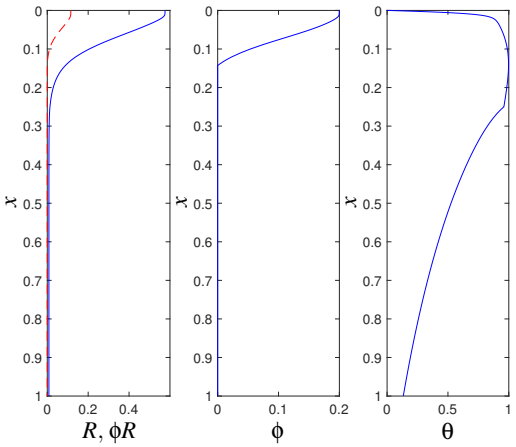

Figure 2: Solution for $p_H=132$ Pa; $T=20.97$, the channel closes so that $\phi_{out}=0$.

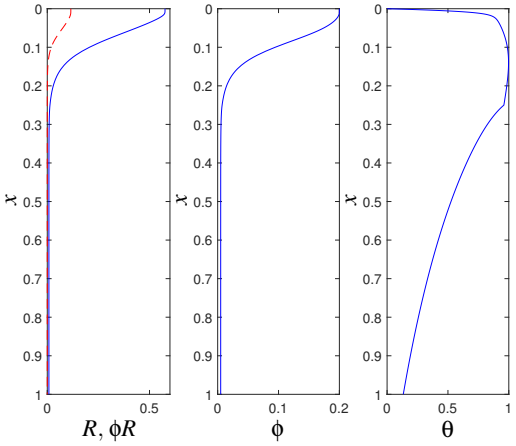

Figure 3: Solution for $p_H=220$ Pa; $T=20.98$, $\phi(x)$ decreases monotonically to $\phi_{out}=0.005$.

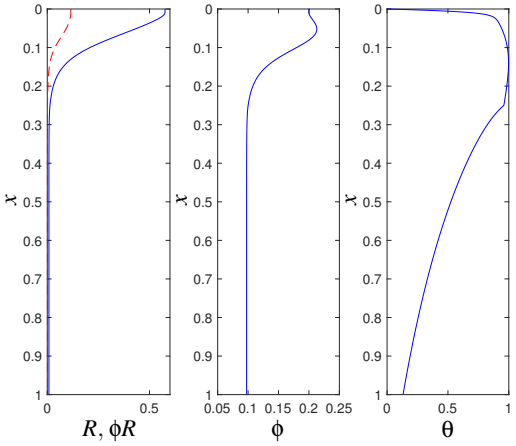

Figure 4: Solution for $p_H=353$ Pa; $T=21.02$, $\phi(x)$ increases at first but then decreases to $\phi_{out}=0.098$.

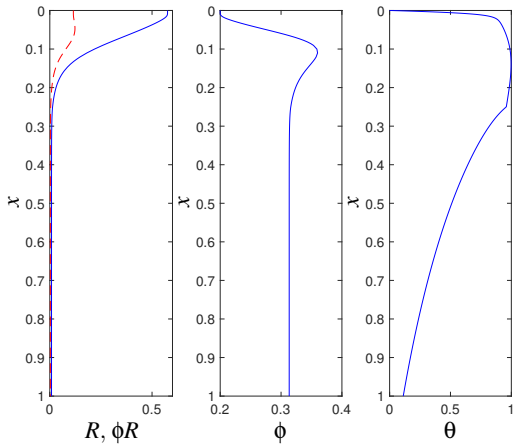

Figure 5: Solution for $p_H = 529$ Pa; $T = 21.21$, $\phi_{out} = 0.31$ and we have $\phi_{out} > \phi_{in}$.

with maximum value θ_{hot} at $x = L_h/2$. The tube was assumed to be made of a glass having $\rho = 3600\,\mathrm{kg\,m^{-3}}$, $c_p = 557\,\mathrm{J\,kg^{-1}K^{-1}}$, $k = 0.78\,\mathrm{W\,m^{-1}K^{-1}}$ and $\gamma = 0.23$ N/m, while the absorptivity was set at $\beta = 0.6$ and the Stefan-Boltzmann constant is $k_b = 5.67 \times 10^{-8}\,\mathrm{W\,m^{-2}K^{-4}}$. The dimensional viscosity-temperature relation was taken to be that for Schott F2 glass, namely [14]

$$\log_{10}\mu = -2.314 + \frac{4065.2}{\theta - 410.15}, \tag{17}$$

where θ is measured in Kelvin and μ is given in Pa s. From this data we find $\varepsilon = 0.043$, $\ell = 0.25$, Pe $= 11.98$, Ca $= 0.166$, $\mathcal{H}_R = 7.97$, $\vartheta_a = 0.29$, $\vartheta_{in} = 0.65$.

For $p_H = 132$ Pa (Figure 2) we see that the pressure is not sufficient to stop the channel from closing and $\phi = 0$ in the final fibre. For $p_H = 220$ Pa (Figure 3), ϕ decreases monotonically but the channel remains open. At the larger value $p_H = 353$ Pa (Figure 4), ϕ initially increases but then decreases so that $\phi_{out} < \phi_{in}$. Finally increasing the pressure still further to $p_H = 529$ Pa (Figure 5) results in a fibre of aspect ratio larger than ϕ_{in}.

Complex cross-sectional geometries

With an appropriate method for solving the transverse-flow model, the extensional-flow model may be solved for initial cross-sections of arbitrary geometry; computational details and some examples may be found in [1, 2, 15]. Here we show in Figure 6, taken from [3], a comparison of the extensional-flow model with experimental results and a 3D finite-element simulation for an initial geometry with 6-holes and an external diameter of 4 mm. The extensional-flow model captures the cross-sectional fibre geometry extremely well and better than the finite-element simulation. This provides excellent validation of the extensional-flow modelling approach for the drawing of slender fibres.

Conclusions

We have described the derivation of an extensional-flow model applicable to the drawing of fibres with, possibly, one or more air channels running along the length of the fibre. Asymptotic methods were used to obtain the model which is comprised of a 2D free-boundary Stokes-flow problem describing the flow and geometry evolution in the cross-section, coupled 1D problems for the axial flow and temperature which, to a good approximation, are uniform in a cross-section. As might be anticipated, the axial-flow model features the Trouton or extensional viscosity which is three times the shear viscosity. We considered deformation of the geometry by stretching, surface tension and pressurisation of air channels. In the absence of surface tension and pressure the cross-sectional geometry reduces in size but does not change in relative shape [5, 6].

For the drawing of an annular tube the model reduced to four coupled ODEs which were solved using a Matlab ODE solver. Solutions showed a competition between surface tension which acts to close air channels and pressurisation of air channels which acts to open them. Depending on the relative strengths of these two forces the aspect ratio of the tube may decrease or increase and, for a sufficiently large pressure, the aspect ratio of the final fibre may be larger than that of the initial cross-sectional geometry.

A comparison of the asymptotic extensional-flow model with experiments and finite-element simulations, for the drawing of a slender fibre with 6 air channels, demonstrated the remarkable accuracy of the asymptotic model. Accuracy deteriorates as the slenderness assumptions become less valid but the model remains useful for fibre drawing where the initial diameter is of the order of a centimetre or so. The model is also very efficient with solution taking much less time than full Navier-Stokes simulations. Each of the solutions shown in this paper took less than five seconds to generate using Matlab on a MacBook Pro with a 2.9 GHz Intel Core i5 processor and 8GB of memory.

The methods illustrated in this paper are also applicable for other extensional flow problems.

Acknowledgements

The author is grateful for the support received from Australian Research Council grants DP130101541 and FT160100108.

References

[1] Buchak, P., Crowdy, D.G., Stokes, Y.M., Ebendorff-Heidepriem, H.: Elliptical pore regularisation of the inverse problem for microstructured optical fibre fabrication. J. Fluid Mech. 778, 5–38 (2015).

[2] Chen, M.J., Stokes, Y.M., Buchak, P., Crowdy, D.G., Ebendorff-Heidepriem, H.: Microstructured optical fibre drawing with active channel pressurisation. J. Fluid Mech. 783, 137–165 (2015).

[3] Chen, M.J., Stokes, Y.M., Buchak, P., Crowdy, D.G., Ebendorff-Heidepriem, H.: Asymptotic modelling of a six-hole MOF. J. Lightwave Technol. 34, 5651–5656 (2016).

[4] Cummings, L.J., Howell, P.D.: On the evolution of non-axisymmetric viscous fibres with surface tension, inertia and gravity. J. Fluid Mech. 389, 361–389 (1999).

[5] Dewynne, J.N., Ockendon, J.R., Wilmott, P.: A systematic derivation of the leading-order equations for extensional flows in slender geometries. J. Fluid Mech. 244, 323–338 (1992).

[6] Dewynne, J.N., Howell, P.D., Wilmott, P.: Slender viscous fibres with inertia and gravity. Q. Jl Mech. appl. Math. 47, 541–555 (1994).

[7] Fitt, A.D., Furusawa, K., Monro, T.M., Please, C.P., Richardson, D.A.: The mathematical modelling of capillary drawing for holey fibre manufacture. J. Engng. Maths 43, 201–227 (2002).

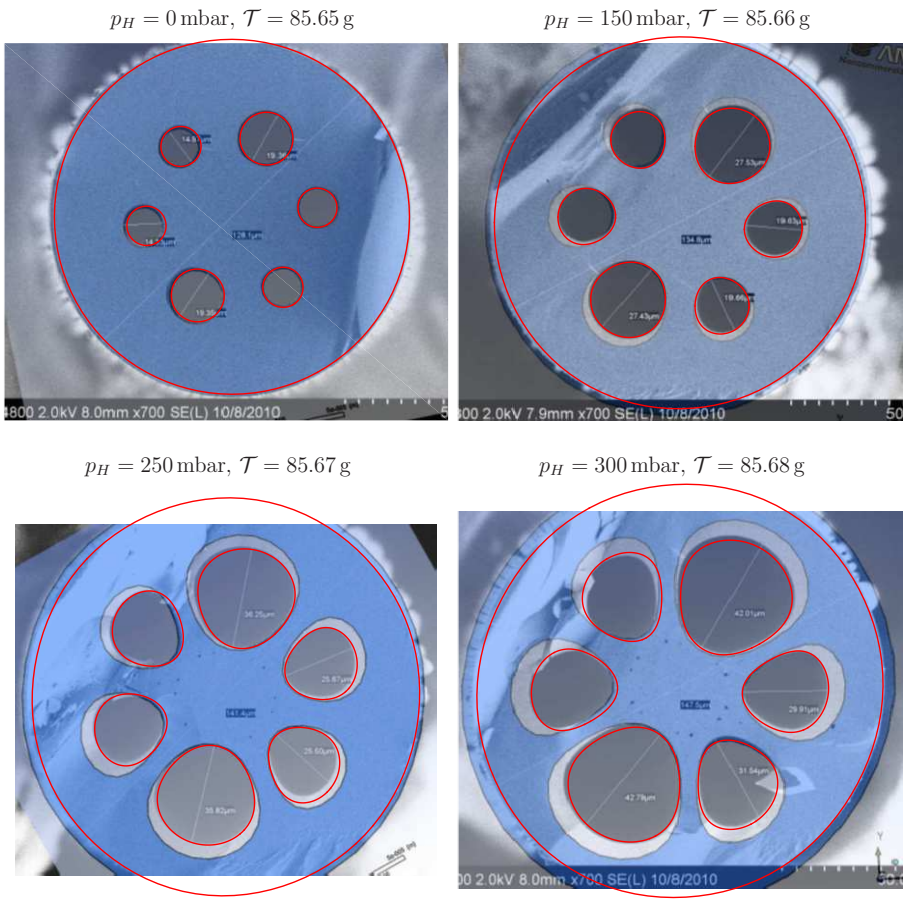

Figure 6: Experimental microscope images of the fibre cross-section, overlaid with the finite element simulation of [9] (pale blue transparency) and the results of the new asymptotic simulation (thin red lines). Shown are the four values of pressurisation from [9, Fig. 3]. For each example the dimensional pressurisation applied is shown in the caption above the image, along with the dimensional fibre tension as calculated by the iterative scheme.

[8] Griffiths, I.M., Howelle, P.D.: Mathematical modelling of non-axisymmetric capillary tube drawing. J. Fluid Mech. 605, 181–206 (2008).

[9] Luzi, G., Epple, P., Scharrer, M., Fujimoto, K., Rauh, C., Delgado, A.: Numerical solution and experimental validation of the drawing process of six-hole optical fibers including the effects of inner pressure and surface tension. J. Lightwave Technol. 30, 1306–1311 (2012).

[10] Matovich, M.A., Pearson, J.R.A.: Spinning a molten threadline; steady-state isothermal viscous flows. Ind. Eng. Chem. Fundam. 8, 512–520 (1969).

[11] Modest, M.F.: *Radiative Heat Transfer*, 3rd ed. Academic Press, 2013, ISBN 978-0-12-386944-9.

[12] Pearson, J.R.A., Petrie, C.J.S.: The flow of a tubular film. Part 1. Formal mathematical representation. J. Fluid Mech. 40, 1–19 (1970).

[13] Pearson, J.R.A., Petrie, C.J.S.: The flow of a tubular film. Part 2. Interpretation of the model and discussion of solutions. J. Fluid Mech. 42, 609–625 (1970).

[14] Richardson, K.: Private communication as part of NSF-DMR #0807016 "Materials world network in advanced optical glasses for novel optical fibers" (2012).

[15] Stokes, Y.M., Buchak, P., Crowdy, D.G., Ebendorff-Heidepriem, H.: Drawing of microstructured optical fibres: circular and non-circular tubes. J. Fluid Mech. 755, 176–203 (2014).

[16] Stokes, Y.M., Wylie, J.J., Chen, M.J.: Coupled fluid and energy flow in fabrication of microstructured optical fibres. In preparation.

[17] Tronnolone, H., Stokes, Y.M.: Pinch-off masses of very viscous fluids extruded from dies of arbitrary shape. Phys Fluids 30, 073103 (2018).

[18] Trouton, F.T.: On the coefficient of viscous traction and its relation to that of viscosity. Proc Roy Soc A 77, 426-440 (1906).

[19] Wilson, S.D.R.: The slow dripping of a viscous fluid. J. Fluid Mech. 190, 561–570 (1988).

[20] Wylie, J.J., Bradshaw-Hajek, B.H., Stokes, Y.M.: The evolution of a viscous thread pulled with a prescribed speed. J. Fluid Mech. 795, 380–408 (2016).